

Article

Mineralogical and Geochemical Characterization of Talc from Two Mexican Ore Deposits (Oaxaca and Puebla) and Nine Talcs Marketed in Mexico: Evaluation of Its Cosmetic Uses

Teresa Pi-Puig ^{1,2,*}, Dante Yosafat Animas-Torices ³ and Jesús Solé ^{1,2} 

¹ Instituto de Geología, Universidad Nacional Autónoma de México (UNAM), Cd. Universitaria, Coyoacán, Mexico City 04510, Mexico; jsol@geologia.unam.mx

² Laboratorio Nacional de Geoquímica y Mineralogía (LANGEM), Universidad Nacional Autónoma de México (UNAM), Cd. Universitaria, Coyoacán, Mexico City 04510, Mexico

³ Facultad de Química, Universidad Nacional Autónoma de México (UNAM), Cd. Universitaria, Coyoacán, Mexico City 04510, Mexico; dante.torices93@hotmail.com

* Correspondence: tpuig@geologia.unam.mx

Received: 1 March 2020; Accepted: 17 April 2020; Published: 26 April 2020



Abstract: The detailed mineralogical, physical and chemical characterization of nine samples of imported cosmetic talc and of two samples of talc from currently non-productive Mexican ore deposits (Oaxaca and Puebla States) is presented. The imported cosmetic talc was classified into two groups, considering whether they are packed in the country of origin or in Mexico and considering their price. X-ray diffraction, infrared short wave, thermogravimetric analysis and scanning electron microscopy were used for mineralogical characterization. For the physical characterization, colorimetry and laser granulometry were used. The chemical composition (major, trace elements) was studied by ICP-MS. It was concluded that only the highest priced and imported in packaged form talcs meet the specific purity requirements for a talc of cosmetic type. The talcs that are packed in Mexico and the talc of the studied Mexican deposits present mineralogical and chemical impurities that make their use difficult in the manufacture of high-quality cosmetic talc. The low-price talc should not be sold as cosmetic talc, and the regulations in Mexico on this subject should be reviewed and updated.

Keywords: clay minerals; industrial minerals; cosmetic talc regulations; SWIR; X-Ray diffraction; mineralogy; colorimetry

1. Introduction

Talc is a hydrous magnesium 2:1 phyllosilicate mineral with a chemical composition of $Mg_3Si_4O_{10}(OH)_2$, which corresponds to a theoretical content of 63.5% of SiO_2 ; 31.7% of MgO and 4.8% of H_2O . Although the composition of talc usually stays close to this formula, some substitutions occur. Small amounts (<2%) of Ca, Fe, Al or Mn can substitute for Mg; and small amounts of Al (2–4% of Al_2O_3) or Ti can substitute for Si [1]. Talc may also contain small quantities of other minerals such as magnesium-aluminum-ferrous silicates (chlorites and fibrous amphiboles), and carbonates (calcite, magnesite, and dolomite). Regarding its structure, talc is monoclinic (C 2/c) or triclinic (C $\bar{1}$) and presents a perfect basal exfoliation. When pure, it has a hardness of 1 to 1.5 on the Mohs scale, a specific weight of 2.75 g/cm³ and a characteristic greasy feel.

Talc can be green, white, gray, brown, or colorless. Its color is clearly related with its purity and defines its commercial grade. Green talc is usually due to the presence of chlorite minerals and dark talc is formed in the presence of organic matter.

Finely ground talc is used as the powder base of many cosmetic products, since it has many interesting properties such as light color, softness, ductility, good luster, lamellar structure with high specific surface area and wide particle size distribution, hydrophobicity (along Si surface), hydrophilicity (fractured along silica-brucite-silica layers), organophilicity, chemical inertness, high lubricant powder, absorption of specific types of oil and fats, heat resistance and high melting point [2–10]. The presence of asbestiform minerals and/or heavy metals reduces their commercial value and their possible applications on cosmetic or pharmaceutical forms [11–13].

Geology and Genesis of Talc Ore Deposits

Geologically, talc is always associated with metamorphic, hydrothermal, or metasomatic processes that have acted on magnesium-rich rocks like dolomites and mafic or ultramafic rocks. The mineralogical and geochemical nature of talc is clearly defined by the host rocks. For this mineral to be formed it is required: (a) to have magnesium rich host rocks; (b) hydrothermal solutions rich in SiO_2 and (c) presence of structures that favor the circulation of fluids [14]. In the deposits associated with mafic or ultramafic rocks the metasomatism is important, and we will find the talc to be associated with important amounts of carbonate. One characteristic reaction of the process is $2(\text{Mg}_3\text{Si}_2\text{O}_5(\text{OH})) + 3\text{CO}_2 \rightarrow \text{Mg}_3\text{Si}_4\text{O}_{10}(\text{OH})_2 + 3\text{MgCO}_3 + 3\text{H}_2\text{O}$. These talcs will be generally rich in iron, nickel and chromium.

For the case of talc formation in dolomites, hydrothermalism must be associated with silica-rich fluids. For example: $3(\text{CaMg}(\text{CO}_3)_2) + 4\text{SiO}_2 + \text{H}_2\text{O} \rightarrow \text{Mg}_3\text{Si}_4\text{O}_{10}(\text{OH})_2 + 3\text{CaCO}_3 + 3\text{CO}_2$ [14].

In Southern Mexico, between the faults of Papalutla and Oaxaca, there are two important metamorphic complexes with small deposits of talc (Figure 1) and magnesite located inside serpentine bodies: (a) Tehuitzingo-Tecomatlán in Puebla, of Paleozoic age, and (b) Cuicatlán-Concepción-Pápalo in Oaxaca, of Cretaceous age [15].

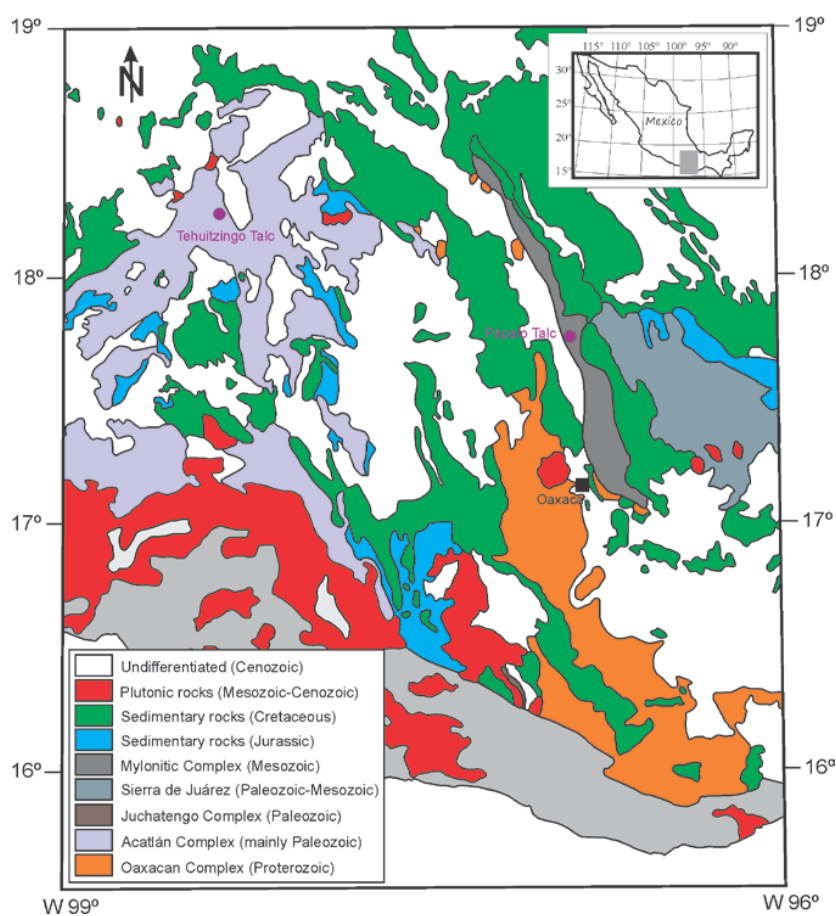


Figure 1. Geological location of the studied talc ore deposits from Mexico. Modified from [16].

In the Tehuiztzingo area, the talc ore deposit is associated with a sequence of basic to ultrabasic serpentinitized rocks (~7 km long, ~0.5 km thick) and probably related to a protolith of harzburgite composition [17]. The serpentinite body consists of chlorite schists, talc and magnesite schists, massive serpentinites (lizardite and antigorite mainly with chromite and magnetite), and ultrabasic dykes [15,17]. In this sequence of rocks, a minimum of two serpentinitization events were identified, the first associated with compressive tectonics and the second (to which talc formation is associated) with a hydrothermal process [15,17].

This basic-ultrabasic body is embedded in a metasedimentary greenschist facies sequence, and the talc outcrops, despite having an irregular distribution, are mainly concentrated in the contact area between the basic-ultrabasic body and the metasedimentary sequences.

Regarding its origin, Ortega-Gutiérrez [18] considered that this serpentinite unit derived from magmatic rocks and should be associated with an allochthonous and dismembered ophiolitic sequence that has more recently been classified as a suprasubduction ophiolite [19].

The Cuicatlán-Concepción Pápalo complex is located in the Cuicateco terrane, which includes oceanic crust and metatuffs, black shales and metacarbonates in greenschist facies of Upper Jurassic-Lower Cretaceous age [20].

In the Concepción Pápalo zone, strongly sheared intrusions of diorites and monzonites define a mylonitic belt associated with serpentinites, with N-NE orientation, a maximum thickness of about 300 m and concordant foliation with the enclosing rocks [16,17,20]. Talc is found associated with the serpentinite bodies, which have been interpreted as the altered ultramafic rocks from the root of a volcanic arc [20].

Mexico produces less than 0.5% of all talc in the world, and currently most of the companies that sell talcum in this country buy it from other countries such as USA, China or Australia which are some of the leading producers in the world. In 2017 and 2018, according to the mining yearbook of the Mexican Geological Service [21], the only states producing talc were Guerrero (89%), Baja California (4.6%), Zacatecas (3.8%) and Guanajuato (2.5%). The production of talc in the country has decreased from 11,392 tons in 2016 to 1280 tons in 2017 and then incremented again to 5917 tons in 2018. There has also been an increase in the importation of talc, so that different companies now buy talc from other countries (mainly USA) and pack it in Mexico selling it as talcum produced in Mexico.

All this leads us to wonder whether talc from some states can be used or not as a raw material for cosmetic products and at the same time review the quality of the different types of talc marketed in the country. Currently, there is no specific standard in Mexico on the quality of a cosmetic talc or a specific protocol to determine whether a talc can be used or not in the manufacture of cosmetic products based on its physicochemical and mineralogical properties. Official Standards (NOM-118-SSA-1994; NOM-199-SSA-2000; NOM-047-SSA-2011) for talc of cosmetic uses indicate that the only requirement is not to contain carcinogenic particles such as asbestos or heavy metals.

The main goal of this work is to characterize the mineralogical and geochemical nature of the talc of two Mexican deposits and compare their quality with respect to talc of different prices (4 of high price and 5 of low-medium price) marketed in this country. It is also intended to review the need to establish new specific regulations to legislate the quality requirements for the cosmetic talc in Mexico.

2. Materials and Methods

2.1. Selection and Preparation of Samples

Representative samples of the Puebla and Oaxaca ore deposits were crushed for 5 min by means of a Micronizing Miller until obtaining about 250 g of homogeneous material.

The nine selected commercial cosmetic talc samples included high (4), medium (3), and low-priced (2) products, in order to test a broad product range; a packaged product of about 200 g of each of the selected trademarks was purchased. The first 4 samples correspond to already packaged cosmetic talc of high price that is imported from other countries and sold abroad. The other 5 samples are

cosmetic commercial talc from medium to low price that is packed in Mexico (states of Nuevo Leon and Chihuahua mainly). All commercial samples did not require a preliminary treatment.

2.2. Colorimetry

For the color quantification, a spectrophotometer model sph860/sph900 (ColorLite GmbH, Katlenburg-Lindau, Germany) was used. Once the equipment was calibrated with a standard, we proceeded to measure the color of each sample (and its respective duplicate) by placing it inside a glass container, always ensuring that the bottom of the holder was totally covered by particles of the sample to avoid the loss of light and the distortion of color that arises from it.

For the purposes of this study, the brightness (L) on a white/black scale (0 a 100) and the red to green (a^*) and yellow to blue (b^*) coordinates (hunter scale) are all considered. Color is determined by pressing the powder into a pellet at standard conditions (3 bar). The b^* value, called also tint, is a critical commercial value and often is related with iron content.

The whiteness index (WI) values were calculated by taking the values of the CIELab scale (L , a^* , b^*) and the Hunter equation [22], modified by Stensby [23]:

$$WI = L - 3b^* + 3a. \quad (1)$$

2.3. X-Ray Diffraction (XRD)

X-Ray diffraction spectra of non-oriented and oriented aliquots [24] have been acquired using an Empyrean diffractometer (Malvern Panalytical, Malvern, UK) operating with an accelerating voltage of 45 kV and a filament current of 40 mA, using $\text{CuK}\alpha$ radiation, nickel filter and a PIXcel 3D detector (Malvern Panalytical, Malvern, UK). Samples were measured in the range of 4° – 80° (2theta) with a step size of 0.002° (2theta) and 90 s of scan step time. Phase identification and quantification by the Rietveld method were made using the Highscore v4.5 software (Malvern Panalytical, Malvern, UK) and ICDD (International Center for Diffraction Data) and ICSD (Inorganic Crystal structure Database) databases.

Because chlorite and serpentine minerals are difficult to differentiate—serpentine has (004) peak at 3.66 Å and chlorite has a major diffraction peak (004) also in this region—the talc with chlorite was heated to 800 °C to destroy chlorite peaks and measured again by XRD to verify the possible presence of serpentine group minerals. The samples were heated to 800 °C because there was no change in the crystal structure of talc or serpentine minerals up to this temperature. At 800 to 840 °C, talc decomposed to enstatite, amorphous silica, and water vapor [25].

A talc XRD morphology index [26], calculated from the XRD data, numerically relates the morphology of the talc to its XRD peak intensities. This index (M) allows us to assign upper and lower limits to the talc texture: they can range from 100% blocky at $M = 0$ to 100% platy at $M = 1$. The index was obtained using the equation:

$$M = I_x / (I_x + 2I_y), \quad (2)$$

where I_x is the intensity of the (004) peak and I_y is that of the (020) reflection (overlapped with the (11-1) and (110) peaks) [26].

2.4. Short Wave Infrared Spectroscopy (SWIR)

The analysis by Short Wave Infrared Spectroscopy was performed for all the samples with a portable OreXpress SM-3500 (Spectral evolution) spectrophotometer (Spectral Evolution, Haverhill, MA, USA) and EZ-ID evaluation software (Spectral Evolution, Haverhill, MA, USA). Before performing the measurement of the samples, a barite blank was measured to calibrate the equipment; this calibration operation was repeated at intervals of every 5 measured samples. Before being analyzed, the samples were gently disaggregated and mounted in a small circular holder to be measured. Each sample was measured two times, to verify the response of the spectrophotometer. At the end of the measurement, the samples were returned to their original containers and stored in the room at 25 °C for later analysis.

2.5. Scanning Electron Microscopy (SEM)

The samples were observed using a scanning electron microscope Olympus BX41 Model HR800 installed in the headquarters of the National Institute of Anthropology and History (INAH) located in the Historic Center of Mexico City. Increases in the range of 500× to 1200×, high vacuum, voltage of 20 kV and data acquisition times of approximately one minute per point were used. The samples were previously lyophilized by a LABONCO instrument in the Laboratory of Environmental Edaphology of LANGEM (National Laboratory of Geochemistry and Mineralogy) at a temperature of 40 °C and a pressure of 0.133 mbar for 18 h.

2.6. Granulometry

A granulometric analysis was carried out using a BECKMAN COULTER analyzer model LS230 with a laser diffraction system installed in the Instituto de Ciencias del Mar y Limnología (ICMyL) of the Universidad Nacional Autónoma de México (UNAM). The equipment measures in a range of from 0.04 microns to 2000 microns. For this analysis, each sample was mixed for 2 min with 20 drops of a 2M solution of sodium hexametaphosphate that acts as a dispersant, since talc is hydrophobic. The equipment was calibrated by means of a water standard curve and the samples were agitated at 60 revolutions per minute during the measurement to avoid the formation of aggregates.

2.7. Chemistry of Whole Rock and Trace Elements by Inductively Coupled Plasma

All talc samples were analyzed by ICP-MS (Inductively Coupled Plasma) at Actlabs laboratories (Canada). A combination of packages Code 4B (lithium metaborate/tetraborate fusion ICP whole rock) and Code 4B2 (trace element ICP/MS) was used. The samples were melted by a flow of lithium metaborate and tetraborate using an induction furnace; once this process was complete, they were continuously mixed with a 5% nitric acid solution containing an internal standard until the sample was completely dissolved.

Diluted samples were analyzed with a Perkin Elmer Sciex ELAN 6000, 6100 or 9000 ICP/MS. Three blanks and five controls (three before sample group and two after) were analyzed with the samples. The method was used for the determination of major, minor and lanthanide group elements.

2.8. Thermogravimetric Analysis

Thermogravimetric analyses were done with a LINSEIS STPA 1600 instrument (Linseis Messgeraete GmbH, Selb, Germany). Samples were weighed in open alumina crucibles, and heating was performed between 25 °C and 1000 °C at a rate of 10 °C min⁻¹ in air atmosphere.

3. Results and Discussion

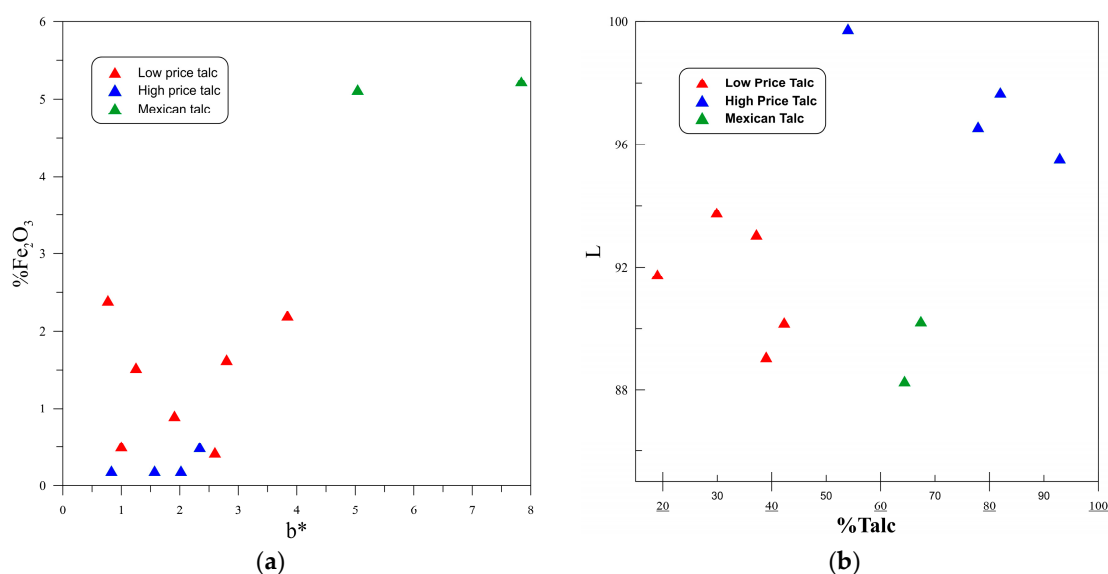
3.1. Color

The talc of Mexican deposits presents luminosity (L) values of 88.28–90.24%; values of a* ranging from −0.05 to 0.66 and values of b* between 5.04 and 7.84.

The high price imported talc samples present luminosity values of 95.6% to 99.8%, values of a* ranging from −0.47 to 0.04 and values of b* between 0.83 and 2.34. The low price imported talc samples present luminosity values of 91.8–97.6% (slightly lower than the values obtained for the higher price talcs); values of a* ranging from −0.26 to 0.20 and values of b* between 1.0 and 3.84 (slightly higher than the values obtained for the high price talcs). A low correlation can be observed between the values of b* with the iron content [27], and a partial correlation between luminosity and the percentage of talc in the sample (Table 1, Figure 2).

Table 1. Colorimetric values of talcs and their relationship with iron content.

Sample	L (%)	a*	b*	Fe ₂ O ₃	WI (%)
Oaxaca	90.24	−0.05	5.04	5.12	75.3
Puebla	88.28	0.66	7.84	5.23	62.8
I	96.57	−0.07	1.57	0.20	92.1
II	97.70	−0.08	2.02	0.20	91.9
III	99.77	−0.47	2.34	0.50	94.2
IV	95.56	0.04	0.83	0.20	93.0
V	93.77	−0.05	1.00	0.51	90.9
VI	91.77	−0.03	1.91	0.90	86.1
VII	93.07	−0.14	1.25	1.53	89.7
VIII	89.07	0.20	2.80	1.63	80.1
IX	90.20	−0.02	2.60	0.43	82.5

**Figure 2.** Correlation between the colorimetric values of b* (tint) and the iron content (a) and between luminosity (L%) and the amount of talc in the sample (b).

The whiteness index ($WI = L - 3a^* + 3b^*$) [23], for high-priced talc is always higher than 91% while for low-priced talc is between 80% and 91%; Mexican talcs are those with a lower whiteness index ($WI < 76\%$).

3.2. Mineralogy by X-Ray Diffraction (XRD)

The talc from Oaxaca (Table 2) consists basically of talc ($\approx 71\%$), chlorite ($\approx 26\%$) and quartz ($\approx 3\%$); carbonates were not detected. Talc from Puebla (Table 2) consists of talc ($\approx 67\%$), chlorite ($\approx 8\%$), quartz ($\approx 5\%$) and dolomite ($\approx 19\%$). The morphological index is ≈ 0.6 for talc from Oaxaca and ≈ 0.8 for talc from Puebla indicating an intermediate (platy and blocky) texture for Oaxaca talc and a predominance of platy texture (Table 3) for Puebla talc.

For high price samples, content of talc is high for three samples (I: 79%; II: 83%; and IV: 90%) and medium ($\sim 50\%$) for sample number III. Based on the Rietveld refinement results, both polytypes of talc (2M and 1A) are present in all samples with predominance of the 2M polytype.

Table 2. Mineralogical composition determined by XRD and refinement by the Rietveld method.

Sample	1A Talc	2M Talc	Cl	Q	Cc	Ma	Do	Clay	Zin	GOF *	Type
Oaxaca	40.0	31.4	26.1	2.6	-	-	-	-	-	1.83	Green-white
Puebla	20.4	47.0	8.3	5.3	-	-	19.0	-	-	1.69	Green-white
I	15.3	63.4	-	5.5	-	-	5.1	3.5	7.2	1.44	White
II	14.6	68.6	5.5	4.1	-	5.9	-	-	1.3	1.93	White
III	32.8	16.7	5.7	9.4	28.0	2.1	1.3	-	4.0	2.28	White
IV	39.6	50.5	-	6.9	-	0.9	1.7	-	0.4	1.09	White
V	28.6	2.7	38.2	13.6	3.1	1.6	6.8	4.1	1.3	1.89	Green
VI	15.6	7.6	49.7	4.4	0.2	15.2	6.5	-	0.8	2.23	Green
VII	27.9	9.3	34.4	20.4	13.9	-	3.7	-	0.4	1.47	Green
VIII	28.2	10.8	29.4	23.6	1.7	-	6.3	-	-	1.53	Green
IX	29.4	10.3	19.8	20.5	6.7	-	12.7	-	-	0.6	Green

1A Talc (ICSD 98-002-1017); Talc 2M (ICSD 98-002-6741); Cl = Chlorite group, clinocllore (ICDD 01-078-1997 and ICDD 01-087-2496); Q = Quartz (ICSD 98-008-3849); Cc = Calcite (ICSD 98-016-9919); Ma = Magnesite (ICSD 98-006-3663); Do = Dolomite (ICDD 01-075-1654); Clay = Clay minerals of smectite (ICSD 98-016-1171) and kaolinite (ICDD 01-078-2110) groups; Zin = Zincite (ICSD 98-005-2362); ICSD = Inorganic Crystal Structure database; ICDD = International Center for Diffraction Data; * GOF = goodness of fitting of the Rietveld refinement.

Table 3. Morphological index [26], of natural Mexican talc from Oaxaca and Puebla ore deposits and cosmetic talc of high and low price.

Sample	FWHM	I(004)	I(020)	(I ₀₀₄ + 2I ₀₂₀)	I _{morphological}
Oaxaca	0.1568	4233	1207	6647	0.6368
Puebla	0.1146	7028	1058	9144	0.7686
I	0.2886	8026	1685	11396	0.7043
II	0.1448	8727	2175	13077	0.6677
III	0.1886	9501	565	10631	0.8937
IV	0.1734	9321	669	10659	0.8744
V	0.1488	2024	4889	11802	0.1715
VI	0.1536	1948	1800	5548	0.3156
VII	0.3262	626	526	1678	0.3731
VIII	0.2759	610	1604	3818	0.1598
IX	0.2331	813	1499	3811	0.2133

The morphological indices (Table 3) are high (0.7–0.9) from what can be deduced that the morphology of crystals is mainly of the platy type with a small proportion of blocky texture. All samples of this group have moderate amounts of quartz (<10%) and for talcum III a quarter of the product are carbonates. All the high price talcs include zincite (ZnO_2).

Talc content in products of low price is always low ranging from 23% (VI) to 40% (IX). The content of chlorite is high and ranges from ~20% (IX) to ~50% (VI). Talc polytype 1A predominates in all samples. All samples have other impurities such as carbonates (from 8% in VII and VIII to 22% in VI) and, with the exception of sample VI (very rich in chlorite and carbonates), considerable proportions of quartz (from 14% in V to 24% in VIII) which determine that low-priced talc is most likely unsuitable for cosmetic use given the hardness and abrasiveness of this mineral. The morphological indices (Table 3) are low or very low (0.2–0.4), from which a predominance of the texture in blocks can be deduced.

The mineralogical differences between the three types of talcs (Mexican, high-priced and low to medium-priced) can be observed by comparing the X-ray diffraction patterns in Figure 3. None of the studied samples contain asbestiform minerals detectable by X-ray diffraction [28].

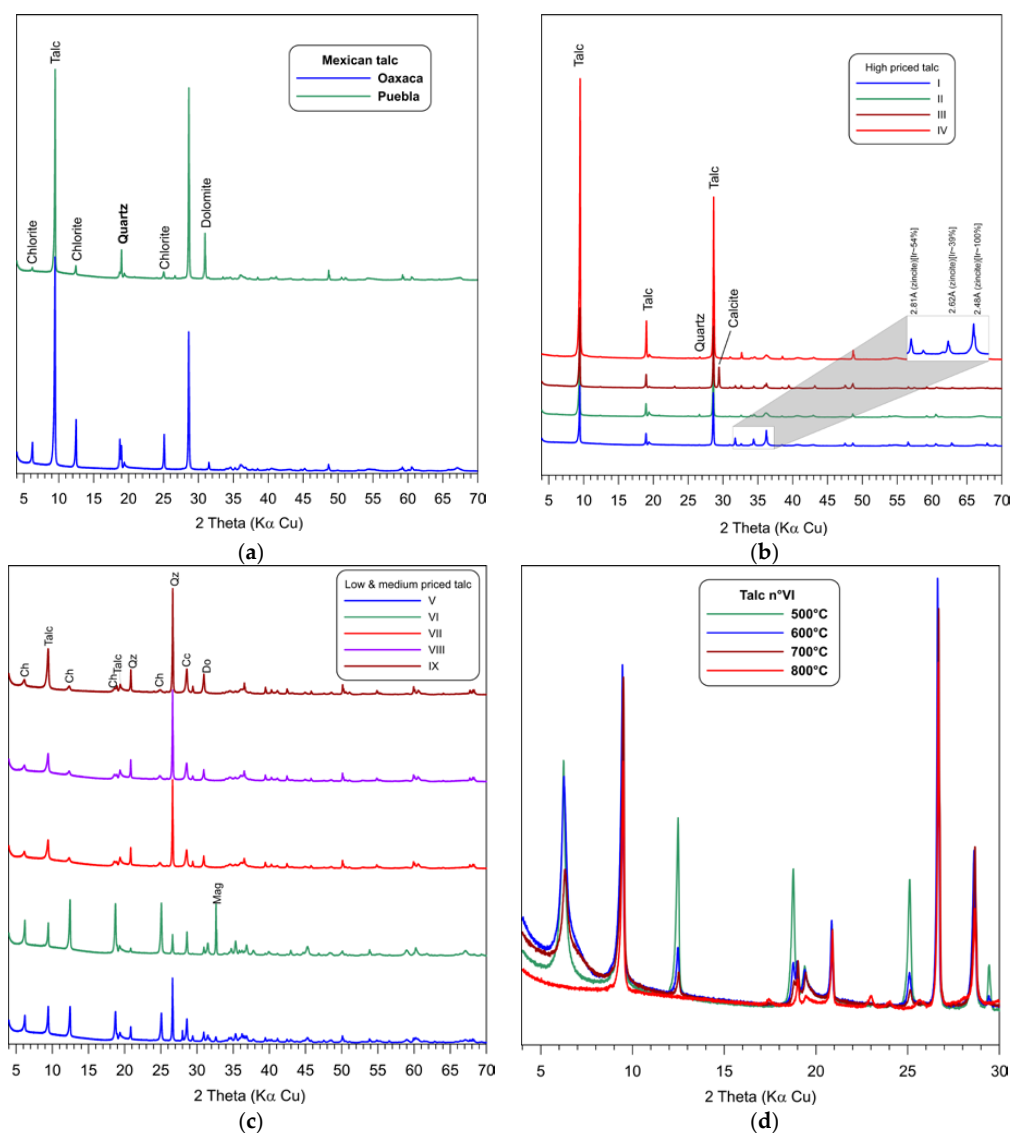


Figure 3. X ray diffraction patterns of three types of talcs: Mexican talc (a), high-price imported talc (with zincite) (b) and low-medium-price imported talc (c). (d) Talc VI heated at different temperatures (500–800 °C) to discriminate chlorite and serpentine group minerals.

Correlating the mineralogy with the price of the product, a very good positive correlation between the content of talc and the price of the product is observed (Figure 4a). In the case of Mexican talc deposits, the price that would imply exploiting these deposits has been calculated approximately. A positive correlation between talc content and morphological index [26], measured by X-ray diffraction, can also be observed (Figure 4b).

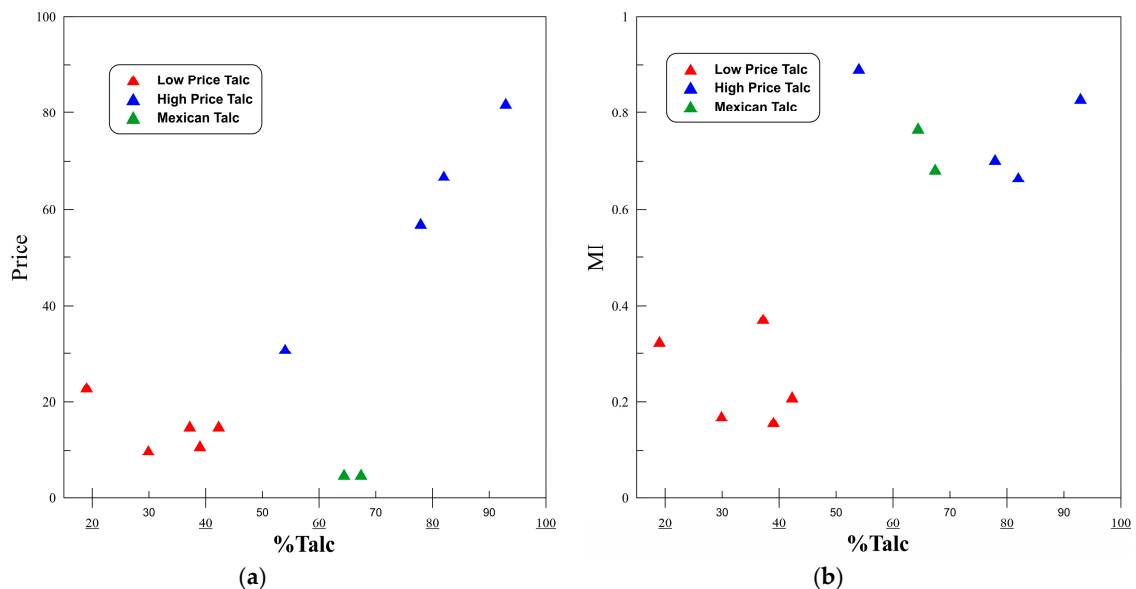


Figure 4. Correlation between price (a), morphological index (MI) (b) and talc concentration in different types of talc.

3.3. Mineralogy by Short Wave Infrared Spectroscopy (SWIR)

Talc is identified by a characteristic doublet at 2320 nm (two bands located at 2300 and 2279 nm); the third major absorption band is located at 2380 nm. Furthermore, and only for the high-quality talc, a triple feature is observed (2077, 2127 and 2172 nm).

Chlorite-dominated spectra are characterized by two important absorption features, centered around 2250 and 2340 nm, caused by Fe–OH and Mg–OH bond stretching respectively [29]. A third feature occurs at around 2000 nm, but this is masked by a large feature at 1910 nm, present in all samples, that is attributable to the presence of molecular water. A feature at around 1400 nm, caused by OH⁻ [30], is consistently present in all the samples.

Carbonates were identified by the bands at 2340 and 2300 nm (superimposed with an important talc band). An absorption feature at around 2195 nm is probably a result of the presence of clay minerals containing Al–OH groups [29].

The spectrum of infrared emission (SWIR) for talc I (high priced) presents a correlation of 0.998 in respect to the pattern of talc found in the database of the United States Geological Survey (USGS). The spectrum of infrared emission (SWIR) for talc from Puebla presents a correlation of 0.988, while talc VIII (low-priced) has only a correlation of 0.894 with respect to the USGS pattern of talc. The spectrum V (low-priced) has a correlation of 0.941 with respect to the USGS chlorite pattern (higher than for talc).

Absorption bands (Figure 5) are due to the vibrations of the H₂O, OH, FeOH, MgOH, CO₃ and Al–OH molecules.

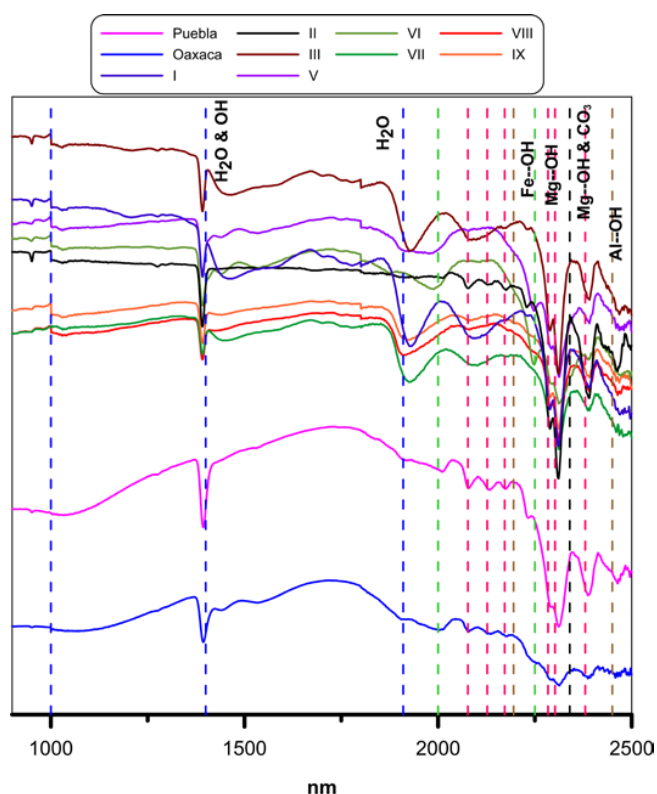


Figure 5. SWIR absorption bands for different types of talcs. In red, bands associated to talc; in green, bands associated with chlorite; in blue, bands associated to water and in brown, bands associated with Al-OH and probably with clay minerals.

The observation by SEM (Figure 6) was used in all samples to verify the possible presence of asbestiform minerals (serpentine or amphiboles) that were never observed. For the talc of Mexican ore deposits, SEM was also used to recognize the morphology [31] of the particles, trying to correlate this data with the morphological index [27] obtained by X-ray diffraction analyses.

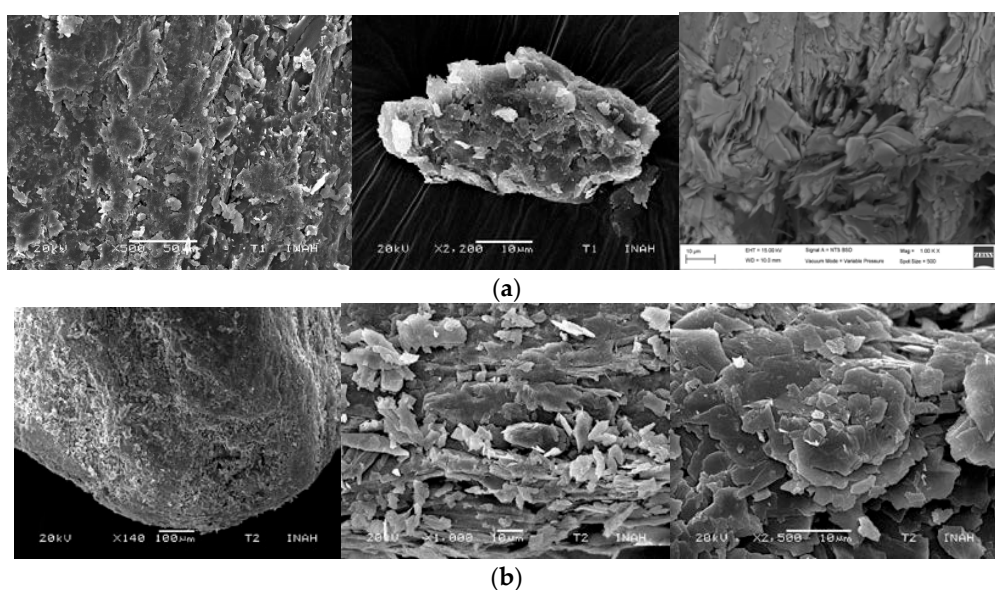


Figure 6. Dimensions and morphology of crystals and aggregates of Mexican talcs observed by SEM. (a) Oaxaca talc with intermediate platy morphology related with a morphological index of 0.6; (b) Puebla talc with predominant platy morphology related with a morphological index of 0.8.

Talc from Oaxaca displays heterogeneous aggregates and equidimensional crystals with irregular edges and variable size (2–10 μm), which can also be distinguished in the talc from Puebla. Individual crystals have diameters of 3–15 μm and average thickness of less than 0.5 μm .

In both Mexican talcs (Oaxaca and Puebla), we have a similar granulometric distribution (Table 4), with a predominance of silt (86–88%) and a percentage of clays ranging from 9% to 12%. Meanwhile, the percentage of sand-sized particles is less than 3%.

Table 4. Grain size distribution (%) of natural Mexican talc from Oaxaca and Puebla ore deposits and high and low-priced packed products.

Sample	Sand	Silt	Clay
	(62–2000 μm)	(4–62 μm)	(<4 μm)
Oaxaca	1.4	86.7	11.9
Puebla	2.8	87.7	9.5
I	3.5	86.9	9.6
II	3.0	88.2	8.7
III	1.0	88.4	10.6
IV	3.8	85.0	11.2
V	0.15	82.4	17.5
VI	0.17	82.2	17.7
VII	0.18	78.8	21.0
VIII	-	76.2	23.8
IX	0.72	87.2	12.1

In the four high-priced imported talc samples, a similar grain size distribution was observed, presenting a predominance of silts (86–89%) and a percentage of clays ranging from 9% to 12%, with less than 4% being sand-sized particles. The distribution of sizes is very similar to that observed for talc from Mexican deposits. For all the talcs in the low-medium priced group, a lower proportion of sand-sized particles (0–1%) and a higher proportion of clays (12–24%) were observed than for higher quality talcs. The percentage of silts is generally lower (76–87%) than the one reported for higher quality talcs.

3.4. Thermal Behavior (TG)

Thermogravimetric analysis of all talc samples is shown in Figure 7. For low-priced talc (V, VI, VII, VIII), Puebla talc and sample III, the mass loss between 650 and 800 $^{\circ}\text{C}$ is mainly related with the CO_2 removed from the structure of carbonates. The mass loss at temperature ranges of 500–600 and 760–780 $^{\circ}\text{C}$ (Puebla, Oaxaca, V, VI, VII, VIII and, in low amount, sample II) resulted from the dihydroxylation reaction of chlorite group minerals [25] and disappeared with increasing talc contents in the samples.

The talc used in cosmetics should have less than 7% loss on ignition values [1], and this fact is only fulfilled by three (I, II and IV) high-priced samples. However, for commercial talc we must consider that the presence of flavoring substances and other organic additives can result in ignition losses greater than expected for unprocessed talc.

From 800 $^{\circ}\text{C}$ onwards, we can observe the loss of mass associated with the decomposition of talc, as this temperature the transformation of talc to enstatite (MgSiO_3) and silica minerals (SiO_2) [32–34] begins. Grinding during the preparation of commercial talc products can decrease the bond energy of the OH group linked to Mg and its reactivity because of size reduction [35]. As a result, the decomposition of talc is observed in some samples (VIII) at lower temperature.

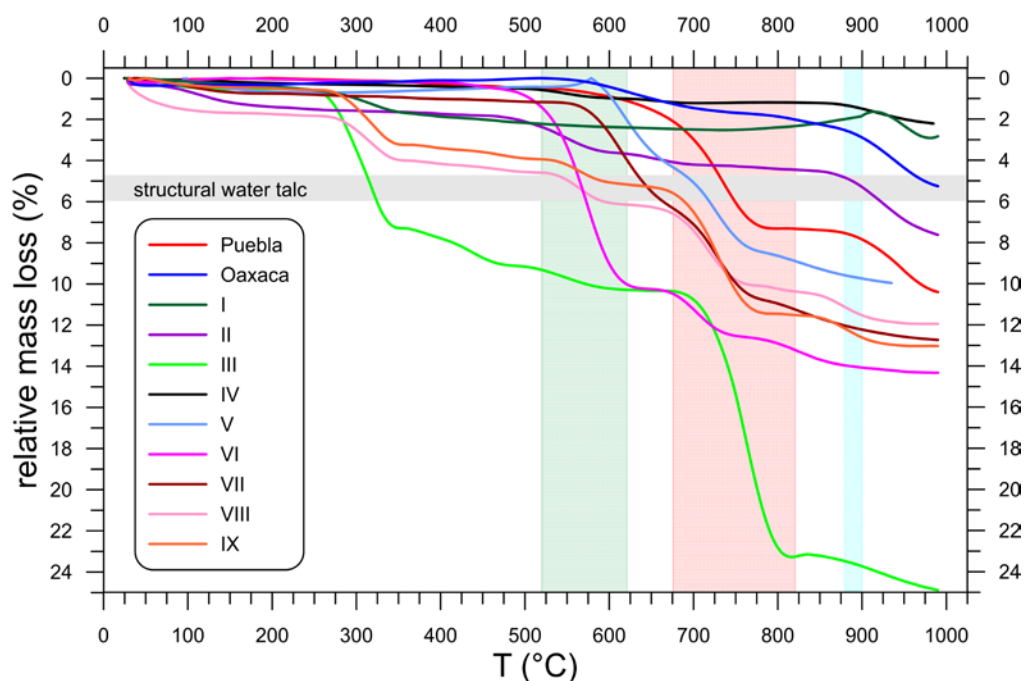


Figure 7. Thermogravimetric (TG) curves for different types of talc. Mass losses associated with carbonate (red), chlorite (green) and decomposition of talc (blue) were drawn as shaded bands.

3.5. Geochemistry of Major, Trace and Lanthanide Elements

Regarding its composition of major elements (Table 5), we can observe that both Mexican talc samples (Oaxaca and Puebla) are slightly poorer in silicon and magnesium than pure talc [1]. Both also present an enrichment in aluminum and iron (associated with the presence of chlorite group minerals or non-crystalline iron oxides that were not detected by X-ray diffraction), e.g., [10]. Moreover, the Puebla talc has more calcium (associated with the presence of carbonates).

In comparison with two high-grade talc ore deposits, samples II and III presented a deficit of silica. All samples in this group are depleted in magnesium in respect to the samples used as reference samples. In sample III, the high content of calcium is related to the presence of carbonates (dolomite) also determined by XRD.

All low-priced talc samples have excess aluminum (especially samples V and VI) and iron (especially samples VII and VIII), which are mainly related to the presence of chlorites but also with mica clay minerals (V) and probably non-crystalline phases with aluminum (VI). Significant deficit of silica for samples VI and IX, despite the presence of quartz, can be observed in Table 5. The loss on ignition (LOI) values of low-priced talcs are always high (13–24%) and related to the presence of carbonates and other clay minerals (chlorite and mica). This is also true for samples VII and IX with important contents of flavoring products.

Regarding trace elements that could be potentially toxic (PET) or harmful (Table 6), we should point out that the two Mexican talcs have high concentrations of chromium (Oaxaca: 1360 ppm; Puebla: 2280 ppm), nickel (Oaxaca: 1440 ppm; Puebla: 1480 ppm) and cobalt (Oaxaca 40 ppm; Puebla: 46 ppm). However, lead (<5 ppm) and arsenic (<4 ppm) were not detected.

Table 5. Major element composition of natural Mexican talc from Oaxaca and Puebla ore deposits and high and low-priced packed products determined by XRF and its comparison with two high-grade talc ore deposits [1]. LOI = loss on ignition.

Sample	SiO ₂	Al ₂ O ₃	MgO	MnO	Fe ₂ O ₃	CaO	NaO	K ₂ O	TiO ₂	P ₂ O ₅	LOI	TOTAL
Australia (Seabrook)	61.9	0.28	31.4	-	-	0.33	0.01	<0.01	-	-	6.05	100
China (Hiachen)	63.5	0.06	31.5	-	-	0.25	0.01	<0.01	-	-	4.91	100.5
Oaxaca	54.79	3.66	29.15	0.03	5.12	0.04	0.02	<0.01	0.01	0.01	6.01	98.84
Puebla	49.31	0.95	26.16	0.10	5.23	4.97	<0.01	<0.01	0.01	0.01	11.3	98.04
I	61.66	1.87	25.02	<0.01	0.31	0.44	0.06	<0.01	<0.01	0.08	8.93	98.37
II	59.92	0.44	31.15	<0.01	0.08	0.49	0.01	<0.01	0.01	0.11	7.28	99.49
III	44.91	0.45	19.45	<0.01	0.06	15.64	0.03	<0.01	<0.01	0.07	16.2	96.81
IV	64.96	0.08	29.32	<0.01	0.17	0.21	0.01	<0.01	<0.01	0.04	5.13	99.92
V	46.99	8.05	25.36	0.03	0.92	3.13	0.02	0.09	0.11	0.06	13.3	98.06
VI	35.82	14.01	31.43	0.01	0.51	1.22	0.01	0.18	0.17	0.03	15.9	99.29
VII	51.35	2.48	17.03	0.05	1.33	4.08	0.04	0.01	0.01	0.08	20.7	97.16
VIII	57.72	3.16	21.72	0.05	1.62	3.3	0.03	0.01	<0.01	0.09	11.9	99.60
IX	48.25	4.03	20.09	0.01	0.43	1.19	0.03	0.04	0.06	0.07	24.3	98.50

Table 6. Minor element composition (ppm) of natural Mexican talc from Oaxaca and Puebla ore deposits and high and low-priced packed products, determined by ICP-MS. The zinc content is related to the presence of the mineral zincite that is used as a colorant in the packaged samples.

Sample	Cr	Ni	Cu	As	Mo	Co	Sn	Sb	Ta	W	Pb	Bi	Th	U	V	Be	Zr	Ba	Zn
Oaxaca	1360	1440	<10	<5	<2	40	<1	0.7	<0.01	<0.5	<5	<0.1	<0.05	0.04	37	<1	4	12	-
Puebla	2280	1480	20	121	<2	46	<1	0.8	0.14	<0.5	11	<0.1	<0.05	0.16	26	<1	4	554	-
I	<20	<1	<10	<5	<2	<1	<1	0.2	<0.01	<0.5	<5	<0.1	0.15	3.22	7	<1	10	4	>10,000
II	<20	<1	<10	<5	<2	<1	<1	0.2	0.07	<0.5	6	<0.1	0.25	5.29	10	<1	10	3	3793
III	<20	<1	<10	<5	<2	<1	<1	1.3	<0.01	<0.5	<5	<0.1	0.09	1.32	7	<1	9	10	>10,000
IV	-	-	-	-	-	-	-	-	-	-	-	-	-	-	-	-	-	-	-
V	<20	<20	10	<5	12	1	<1	0.3	0.15	0.6	67	0.4	1.72	1.46	28	<1	65	630	9000
VI	20	<20	<10	<5	<2	1	<1	<0.2	0.27	1.3	5	<0.1	2.7	1.12	22	<1	105	9	4480
VII	<20	<20	10	<5	43	<1	<1	0.5	<0.01	18.5	172	0.4	<0.05	1.54	40	<1	8	1183	>10,000
VII	<20	<20	<10	<5	26	<1	<1	0.3	<0.01	<0.5	144	<0.1	<0.05	1.57	47	<1	5	1790	860
VIII	-	-	-	-	-	-	-	-	-	-	-	-	-	-	-	-	-	-	-
IX	<20	<20	<10	<5	4	<1	<1	<0.2	<0.01	<0.5	12	<0.1	0.79	0.74	15	<1	31	187	90

For the high-priced imported talcs, we must emphasize that all samples in this group have less than 20 ppm of chromium and nickel, less than 10 ppm of copper, less than 5 ppm of arsenic, less than 2 ppm of molybdenum and less than 1 ppm of cobalt, tin and antimony. The contents of lead (<5 ppm), vanadium (7–10 ppm), tungsten (<0.5 ppm) and barium (<10 ppm) are also low (Table 6).

In regards to trace elements that could be potentially toxic or harmful, it is important to highlight that low-priced talc samples have less than 20 ppm of chromium and nickel, less than 10 ppm of copper, less than 5 ppm of arsenic, less than 2 ppm of molybdenum and less than 1 ppm of cobalt, tin and antimony. However, it is noteworthy that they have a higher content of lead (5–172 ppm), barium (9–1800 ppm) and vanadium (15–40 ppm). In the case of sample VII, its tungsten content also stands out (18 ppm). Ni, Co and Cr are important elements for the identification of talc origin; the Mexican talcs have high concentrations of these elements because they are associated with ultramafic rocks (Table 6).

The concentrations of the elements of the lanthanide group (Figure 8) were normalized to a chondritic composition [36]. High quality talc is characterized by very low lanthanide contents ($\Sigma\text{REE} < 2$ ppm), while lower priced talc packed in Mexico has higher contents ($4 < \Sigma\text{REE} < 32$ ppm). It is important to mention that these elements are found in the talc's accessory minerals. The differences observed in the lanthanide diagram for the talc of Puebla and that of Oaxaca can be clearly related to the origin of both deposits.

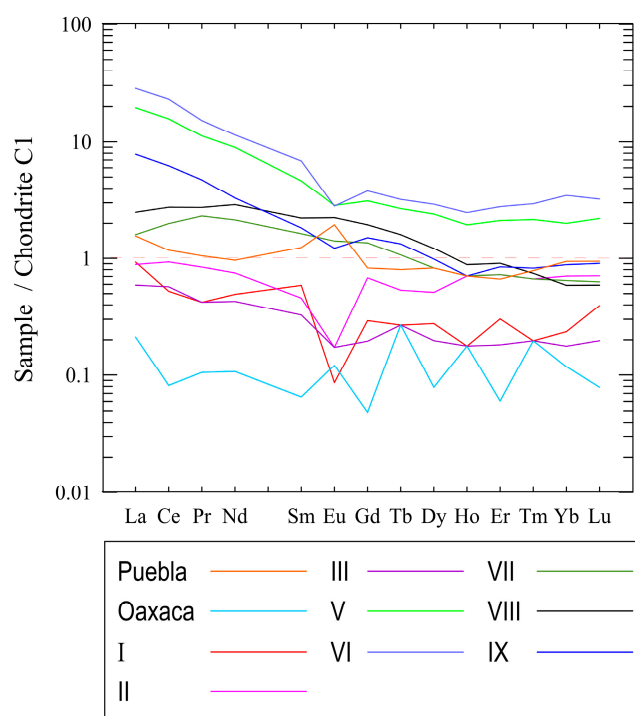


Figure 8. Concentrations of the elements of the lanthanide group in different type of talc normalized to a chondrite C1 [36].

4. Conclusions

SEM observations and high-resolution diffraction routines were used in samples at room temperature and heated to 850 °C to verify the presence of asbestiform minerals in a proportion equal to or greater than 0.5%. Nonetheless, asbestos minerals were not detected in any of the eleven studied samples.

The natural talcs of the ore deposits of Oaxaca and Puebla (Mexico) are not suitable for cosmetic use even though they are quite rich in talc ($\approx 70\%$). They are characterized mostly by a platy morphology (morphological index > 0.6) and have high iron ($> 5\%$ Fe_2O_3), chromium, nickel and cobalt content, related to their genetic relationship with mafic and ultramafic rocks. Both talc ore deposits are

similar, and both have limitations, although it can be considered that Puebla's is of slightly higher quality, despite having an important carbonate content, because its chlorite mineral group content is quite minimal.

The high-priced talc (except for talc III) has proportions of this mineral equal or greater than 75%. Of the highest priced talc, the purest is sample IV (90% of talc); high-priced talc includes impurities of quartz, carbonates (calcite, dolomite, magnesite) and chlorite (less than 6%) that will increase the abrasive strength of talc, but it does not contain harmful or potentially toxic elements (PET). The percentage content in Fe_2O_3 is always less than 0.1%, and the total lanthanides (ΣREE) content is always less than 2 ppm. The morphological indexes are high (0.67–0.89) indicating the predominance of 2M polytype of platy morphology. These brands meet with international regulations about the cosmetic use of this industrial mineral.

The low and medium-priced talc always has talc proportions below 50% (23–40%). The main impurities are chlorites (20–50%), quartz (4–24%), carbonates and clays. The talc polytype 1A predominates as indicated by the low morphological index (0.17–0.37). The contents of iron and aluminum are always higher than higher priced talc but lower than natural talc in Mexico and the high content of Pb, V, W and lanthanides ($\Sigma\text{REE} < 4$ ppm) stand out in these talcs.

The luminosity and tint values (b^*) are partially correlated with the price of the product, but there is not a clear correlation between tint and the iron content of the mineral. Furthermore, the price clearly correlates with the quality of the product. It can be concluded that the low medium-priced talc that is packed in Mexico should not be used for cosmetic use and should be regulated by the law, since mineralogical phases such as chlorite can make up almost 50% of the product even though this information is not indicated on the product labeling. The results also suggest that the morphological index value can be used as a good indicator of product quality coupled with chemical analysis.

Author Contributions: T.P.-P. designed the study and wrote the paper; D.Y.A.-T. and T.P.-P. did the field and laboratory work; J.S. assisted with the writing and the interpretation of the mineralogical, geochemical and physical properties. All authors contributed to data interpretation and discussion. All authors have read and agreed to the published version of the manuscript.

Funding: This research received no external funding.

Acknowledgments: The authors thank Jaime Díaz, Margarita Reyes Salas, Luisa Mainou, Augusto Rodríguez Díaz and Eduardo Morales for their technical support in colorimetric (J.D.), MEB (M.R.S. and L.M.), SWIR (A.R.D.) and granulometric analysis (E.M.).

Conflicts of Interest: The authors declare no conflict of interest.

References

- Galán Huertos, E. *Mineralogía Aplicada*; Síntesis: Madrid, Spain, 2003; ISBN 84-9756-114-7.
- Van Olphen, H. *An Introduction to Clay Colloid Chemistry*; Wiley: New York, NY, USA, 1977.
- Gámiz, E.; Caballero, E.; Delgado Rodríguez, M.; Delgado Calvo-Flores, R. Étude de talcs espagnols à usage pharmaceutique. Composition minéralogique, chimique, propriétés physico-chimiques. *Ann. Pharm. Françaises* **1989**, *47*, 53–61.
- Michot, L.J.; Villiérás, F.; François, M.; Yvon, J.; LeDred, R.; Cases, J.M. The structural microscopic hydrophobicity of talc. *Langmuir* **1994**, *10*, 3765–3773. [[CrossRef](#)]
- López-Galindo, A.; Viseras, C.; Cerezo, P. Compositional, technical, and safety specifications of clays to be used as pharmaceuticals and cosmetic products. *App. Clay Sci.* **2007**, *36*, 51–63. [[CrossRef](#)]
- Wiewióra, A.; Sánchez-Soto, P.J.; Avilés, M.A.; Justo, A.; Pérez-Maqueda, L.A.; Pérez-Rodríguez, J.L.; Bylina, P. Talc from Puebla de Lillo. Spain. I. XRD study. *Appl. Clay Sci.* **1997**, *12*, 233–245.
- Nkoumbou, C.; Villiérás, F.; Njopwouo, D.; Ngoune, C.Y.; Barres, O.; Pelletier, M.; Razafitianamaharavo, A.; Yvon, J. Physicochemical properties of talc ore from three deposits of Lamal Pougue area (Yaounde Pan-African Belt, Cameroon), in relation to industrial uses. *Appl. Clay Sci.* **2008**, *41*, 113–132. [[CrossRef](#)]
- Virta, R.L. Talc and pyrophyllite. In *Mineral Commodity Summaries 2004*; USGS: Reston, VA, USA, 2004.

9. Pialy, P.; Nkoumbou, C.; Villiéras, F.; Razafitianamaharavo, A.; Barres, O.; Pelletier, M.; Ollivier, G.; Bihannic, I.; Njopwouo, D.; Yvon, J.; et al. Characterization for industrial applications of clays from Lembo deposit, Mount Bana (Cameroon). *Clay Min.* **2008**, *43*, 415–435. [[CrossRef](#)]
10. Ersoy, B.; Dikmen, S.; Yildiz, A.; Gören, R.; Elitok, O. Mineralogical and physicochemical properties of talc from Emirdağ, Afyonkarahisar, Turkey, Turk. *J. Earth Sci.* **2013**, *22*, 632–644. [[CrossRef](#)]
11. McCarthy, E.F.; Genco, N.A.; Reade, E.H., Jr. *Industrial Minerals & Rocks: Commodities, Markets, and Uses*; Kogel, J.E., Trivedi, N.C., Barker, J.M., Krukowski, S.T., Eds.; Society for Mining, Metallurgy and Exploration, Inc.: Englewood, CO, USA, 2006.
12. Hu, F.; Gong, N.; Zhang, L.; Lu, Y.; Zhang, P.; Xiao, X.; Liao, L. Quantitative analysis of trace level asbestos in pharmaceutical talc by powder X-ray diffraction. *Anal. Methods* **2014**, *6*, 1862–1867. [[CrossRef](#)]
13. Fiume, M.M.; Boyer, I.; Bergfeld, W.F.; Belsito, D.V.; Hill, R.A.; Klaassen, C.D.; Liebler, D.C.; Marks, J.G., Jr.; Shank, R.C.; Slaga, T.J.; et al. Safety Assessment of Talc as Used in Cosmetics. *Int. J. Toxicol.* **2015**, *34*, 66S–129S. [[CrossRef](#)]
14. McCarthy, E.F.; Genco, N.A.; Reade, E.H., Jr. *Industrial Minerals and Rocks*; Society for Mining, Metallurgy & Exploration: Englewood, CO, USA, 2006; pp. 971–986.
15. Delgado-Argote, L.A.; López-Martínez, M.; York, D.; Hall, C.M. Geologic framework and geochronology of ultramafic complexes of southern México. *Can. J. Earth Sci.* **1992**, *29*, 1590–1604. [[CrossRef](#)]
16. Ortega-Gutiérrez, F.; Mitre-Salazar, L.M.; Roldán-Quintana, J.; Aranda-Gómez, J.; Morán-Zenteno, D.; Alaniz-Alvarez, S.; Nieto-Samaniego, A. *Carta Geológica de la República Mexicana. Escala 1:2,000,000*, 5th ed.; Instituto de Geología: Ciudad de Mexico, Mexico, 1992.
17. Carballido-Sánchez, E.A.; Delgado-Argote, L.A. Geología del cuerpo serpentinitico de Tehuiztingo, Estado de Puebla—interpretación preliminar de su emplazamiento. *Rev. Inst. Geol. UNAM* **1989**, *2*, 134–148.
18. Ortega-Gutiérrez, F. Estratigrafía del Complejo Acatlán en la Mixteca Baja, Estados de Puebla y Oaxaca. *Rev. Mex. Cienc. Geol.* **1978**, *2*, 112–131.
19. González-Mancera, G.; Ortega-Gutiérrez, F.; Proenza, J.A.; Atudorei, V. Petrology and geochemistry of Tehuiztingo Serpentinites (Acatlán complex, SW Mexico). *Bol. Soc. Geol. Mex.* **2009**, *61*, 419–435. [[CrossRef](#)]
20. Delgado-Argote, L.A. Regional implications of the Jurassic-Cretaceous volcanosedimentary Cuicateco Terrane, Oaxaca, Mexico. *Geof. Internac.* **1989**, *28*, 939–973.
21. Mexicano, S.G. *Anuario Estadístico de la Minería Mexicana 2018*; Servicio Geológico Mexicano: Ciudad de México, Mexico, 2018.
22. Hunter, R.S. New Reflectometer and Its Use for Whiteness Measurement. *J. Opt. Soc. Amer.* **1960**, *50*, 44–48. [[CrossRef](#)]
23. Stensby, P.S. Optical Brighteners and Their Evaluation. *Soap Chem. Spec.* **1967**, *97*, 41.
24. Moore, D.M.; Reynolds, R.C., Jr. *X-Ray Diffraction and the Identification and Analysis of Clay Minerals*, 2nd ed.; Oxford University Press: Oxford, UK; New York, NY, USA, 1997.
25. Nkoumbou, C.; Njopwouo, D.; Villiéras, F.; Njoya, A.; Yonta Ngouné, C.; Ngo Ndjock, L.; Tchoua, M.F.; Yvon, J. Talc indices from Boumnyebel (Central Cameroon), physicochemistry and geochemistry. *J. Afr. Earth Sci.* **2006**, *45*, 61–73. [[CrossRef](#)]
26. Holland, H.J.; Murtagh, M.J. An XRD morphology index for talcs: The effect of particle size and morphology on the specific surface area. *Adv. X-Ray Anal.* **2000**, *42*, 421.
27. Soriano, M.; Melgosa, M.; Sánchez-Marañón, M.; Delgado, G.; Gámiz, E.; Delgado, R. Whiteness of Talcum Powders as a Quality Index for Pharmaceutical Uses. *Color Res. Appl.* **1998**, *23*, 178–185.
28. Krause, J.B. Mineralogical characterization of cosmetic talc products. *J. Toxicol. Env. Health* **1977**, *2*, 1223–1226. [[CrossRef](#)]
29. Bishop, J.; Lane, M.; Dyar, M.; Brown, A. Reflectance and emission spectroscopy study of four groups of phyllosilicates: Smectites, kaolinite-serpentines, chlorites and micas. *Clay Min.* **2008**, *43*, 35–54. [[CrossRef](#)]
30. Herrmann, W.; Blake, M.; Doyle, M.; Huston, D.; Kamprad, J.; Merry, N.; Pontual, S. Short Wavelength Infrared (SWIR) Spectral Analysis of Hydrothermal Alteration Zones Associated with Base Metal Sulfide Deposits at Rosebery and Western Tharsis, Tasmania, and Highway-Reward, Queensland. *Econ. Geol.* **2001**, *96*, 939–955. [[CrossRef](#)]
31. Gámiz, E.; Soriano, M.; Delgado, G.; Párraga, J.; Delgado, R. A morphological study of talcs with scanning electron microscopy (SEM): Pharmaceutical applications. *ARS Pharm.* **2002**, *43*, 173–185.

32. Ewell, R.H.; Bunting, E.N.; Geller, R.F. Thermal decomposition of talc. *J. Res. Natl. Bur. Stand.* **1935**, *15*, 551–556. [[CrossRef](#)]
33. Balek, V.; Šubrt, J.; Pérez-Maqueda, L.A.; Beneš, M.; Bountseva, I.M.; Beckman, I.N.; Pérez-Rodríguez, J.L. Thermal behavior of ground talc mineral. *J. Min. Metall.* **2008**, *44B*, 7–17. [[CrossRef](#)]
34. Földvári, M. Handbook of thermogravimetric system of minerals and its use in geological practice. *Occas. Pap. Geol. Inst. Hung.* **2011**, *213*, 1–180.
35. Sánchez-Soto, P.J.; Wiewióra, A.; Avilés, M.A.; Justo, A.; Pérez-Maqueda, L.A.; Pérez Rodríguez, J.L.; Bylina, P. Talc from Puebla de Lillo, Spain. II. Effect of dry grinding on particle size and shape. *Appl. Clay Sci.* **1997**, *12*, 297–312. [[CrossRef](#)]
36. McDonough, W.F.; Sun, S.S. The Composition of the Earth. *Chem. Geol.* **1995**, *120*, 223–253. [[CrossRef](#)]



© 2020 by the authors. Licensee MDPI, Basel, Switzerland. This article is an open access article distributed under the terms and conditions of the Creative Commons Attribution (CC BY) license (<http://creativecommons.org/licenses/by/4.0/>).